論文 / 著書情報
Article / Book Information

Title	The role of autochthonous organic matter in radioactive cesium accumulation to riverine fine sediments
Authors	Manabu Fujii, Keisuke Oono, Chihiro Yoshimura, Manami Miyamoto
Citation	Water Research, Vol. 137, pp. 18-27
Pub. date	2018, 6
DOI	http://dx.doi.org/10.1016/j.watres.2018.02.063
Creative Commons	See next page.
Note	This file is author (final) version.

License

Title

The Role of Autochthonous Organic Matter in Radioactive Cesium Accumulation to Riverine Fine Sediments

Manabu Fujii[†,*], Keisuke Ono[†], Chihiro Yoshimura[†], Manami Miyamoto[†]

† Department of Civil and Environmental Engineering, Tokyo Institute of Technology, 2-12-1-M1-4 Ookayama, Tokyo 152-8552, Japan

* Corresponding author: fujii.m.ah@m.titech.ac.jp

Abstract

Anthropogenically released radioactive cesium (RCs) poses serious ecological and environmental concerns given its persistency in the environment. Although accumulation of RCs in aqueous and sedimentary environments is often reported to associate with organic matter (OM), the mechanisms responsible remain unclear. Here, we investigated RCs in fine sediments along the Abukuma River, the largest river near the Fukushima Daiichi Nuclear Power Plant, 1.5 to 4 years after the accident. Measuring the density-separated sediment fractions with a broad range of OM content (%) indicated that the RCs concentration ($Bq \cdot kg^{-1}$) is positively correlated with OM content for intermediate-density fractions in which OM is primarily characterized by autochthonous origin. This relationship, however, did not hold for light-density fractions containing a high proportion of large-size allochthonous OM. Furthermore, H_2O_2-assisted OM digestion and amorphous material dissolution treatments resulted in only a minor reduction in sedimentary RCs. These results along with the fact that sediments with high autochthonous OM content showed high specific surface area indicated that RCs is tightly associated with finer-grained and chemically non-labile inorganic fractions concurrently resident with autochthonous OM. Overall, our findings highlight that autochthonous OM exerts a significant control on the accumulation, transport, and fate of RCs in aqueous and sedimentary environments.

1. Introduction

The Fukushima Daiichi Nuclear Power Plant (FDNPP) accident on March 11, 2011 resulted in the tremendous release of a range of radionuclides, including 137-Cs, 134-Cs, 131-I, and 90-Sr into the environment(Kinoshita et al. 2011, Kusakabe et al. 2013, Steinhauser et al. 2013, Yasunari et al. 2011). The leakage of radioactive cesium (RCs; 137-Cs and 134-Cs) was estimated to be on the order of 10^{16} Bq(Nuclear Emergency Response Headquarters Government of Japan 2011). The long half-life (~30 years for 137-Cs) and persistence of RCs in a range of aqueous and soil environments indicates that contamination poses serious ecological, environmental, and social problems(Mizuno and Kubo 2013, Murakami et al. 2014, Nakai et al. 2015).

RCs has a high affinity for clay minerals, and thus the majority of RCs deposited on the terrestrial surface environment in Fukushima Prefecture was retained in the upper layer of soil, within a depth of ~5 cm for paddy field sites(Lepage et al. 2015, Matsuda et al. 2015) and in the surface litter layer for forest soil(Koarashi et al. 2012). While a large portion of deposited RCs in the catchment around FDNPP remains in the terrestrial environment (e.g., 1.6% wash-off in the Kuchibuto River watershed by the end of 2014)(Wei et al. 2017b), terrestrial RCs has been gradually transported to reservoirs, rivers, and environments further downstream(Wei et al. 2017a, Yamaguchi et al. 2012, Yamashiki et al. 2014, Yoshimura et al. 2014). In freshwater affected by the FDNPP accident, particulate RCs, such as that associated with fine suspended particles, was dominant in riverine RCs transport according to field surveys performed several years after the accident(Nagao et al. 2013,

Sakaguchi et al. 2015, Tanaka et al. 2015, Yamashiki et al. 2014, Yoshimura et al. 2014), though dissolved RCs has been also detected. In the river waters of the Abukuma River basin, for example, dissolved RCs (<0.45 μm, almost exclusively Cs^+) accounted for 1.2–49% of the total RCs with a spatiotemporal average of 20% from June 2011 to December 2012(Sakaguchi et al. 2015).

After the global fallout due to the Chernobyl accident and nuclear weapons tests, a number of studies on the environmental mobility, bioavailability, and fate of RCs, including adsorption and fixation to clay minerals, have been published. Laboratory-based studies of the interaction of Cs with clay minerals generally suggested that Cs is fixed in specific interlayers of minerals and in layer edge sites, including frayed edge sites, and that it is also retained non-specifically on the surface of planar sites(Bostick et al. 2002, Cornell 1993, Kim et al. 1996a, Kim et al. 1996b, Sawhney 1966). In particular, Cs adsorption to micaceous minerals, such as illite(Comans et al. 1991, Comans and Hockley 1992, Kim et al. 2007) and vermiculite(Bostick et al. 2002, Fan et al. 2014, Kogure et al. 2012), is highly selective, as dehydrated Cs ion is structurally fixed in the interlayers, with some studies suggesting that this fixation reaction may be almost irreversible under specific conditions(Comans et al. 1991, Mukai et al. 2016). Regarding the FDNPP-derived RCs, Mukai and co-workers found that RCs were selectively and uniformly retained on porous weathered biotite (partially vermiculitized biotite) in litter soil(Mukai et al. 2014).

While clay minerals are considered important carriers for RCs in natural aqueous systems, there are accumulated evidence that RCs concentrations in coastal marine (offshore region of FDNPP

and Wuljin Nuclear Power Plant, Korea) and river sediments (six coastal river catchments close to FDNPP) are positively related to organic matter (OM) content(Ambe et al. 2014, Kim et al. 2007, Naulier et al. 2017, Ono et al. 2015). Since alkali metals, including Cs, negligibly form complexes with OM due to the lack of coordination of these metal classes with acidic functional groups, the direct association of RCs with metal binding sites in sedimentary OM is unlikely. Rather, the higher accumulation of RCs in the OM-rich sediment may be related to the grain size and surface area of sediment particles, mineral composition, or combinations of these factors (Ambe et al. 2014, Kim et al. 2007), given that organic and mineral interactions in sediment have been elaborated by the OM-mediated cross-linkage of fine particles(Bock and Mayer 2000) in addition to patch-type coverage of OM primarily at the edge sites of minerals(Mayer 1999). Previous studies indicated the high accumulation of RCs in the smaller size fractions of soil and suspended sediments(Ambe et al. 2014, He and Walling 1996, Sakaguchi et al. 2015, Tanaka et al. 2015). In addition, organic carbon concentrations in riverine and marine sediments are highly correlated with the unit mass-normalized surface area of sediment determined by gas adsorption(Bergamaschi et al. 1997, Hedges and Keil 1995, Keil et al. 1997).

However, the mechanisms behind the RCs accumulation in OM-rich particles remain unclear. Understanding the association of RCs with OM is of importance, given that presence of OM affects to the mobility and bioavailability of RCs in aqueous and sedimentary environments (e.g., Staunton et al., 2002). Since autochthonous OM is a major energy source for freshwater organisms such as grazing

92 fish, sedimentary RCs associated with autochthonous OM can be highly bioavailable and exhibit
93 dynamic behavior in freshwater environments and ecosystems (Fukushima and Arai 2014). In this
94 study, therefore, we investigated the interaction of FDNPP-derived RCs and riverine sediment with
95 particular attention given to the characterization of sedimentary OM including whether it is
96 allochthonous or autochthonous. Suspended and deposited fine sediments <2 mm in size were
97 collected at several sampling stations along the main stream of the largest river near the FDNPP, the
98 Abukuma River (**Figure S1 in Supplementary Material SM 4**), during summer and winter from 2012
99 to 2015. The dried sediment samples were then subjected to various physicochemical treatments (e.g.,
100 density-based separation, H_2O_2 treatment for OM digestion) and subsequent sediment property
101 analyses to examine the relationships among the RCs concentration, OM content, and other sediment
102 properties (e.g., specific surface area). In particular, the characteristics of density-fractionated
103 sediments with different degrees of OM proportions were extensively examined. Nitrogen-to-carbon
104 ratio (N/C ratio) analyses of the sediment samples and end-member samples from the Abukuma River
105 basin (e.g., terrestrial plants, soil OM and riverine algae) were used to identify the source of
106 sedimentary OM. **Figure S2** shows an overview of this study, including sample collection, treatment
107 and analyses.
108
109 **2. Materials and Methods**
110 Detailed information on the general procedure, H_2O_2 treatment, sample analyses, statistical

analyses and fundamental water quality measurement is available in **Supplementary Material (SM 1)**.

2.1 Sample collection

The Abukuma River has a basin area of approximately 5,400 km^2, a total main stream channel length of ~240 km, and a flow rate of 117 $m^3 \cdot s^{-1}$ (averaged over 1966–2009 at Tateyama observation station). The river originates in Asahidake Mountain in the south of Fukushima Prefecture, passes through Fukushima City which is approximately 60 km northwest of FDNPP and finally flows into the Pacific Ocean in Watari City, Miyagi Prefecture.

Deposited fine sediments were collected at several sites in the main stream channel of Abukuma River (St. 1 Watari, St. 2 Marumori, St. 3 Yahata, St. 4 Fukushima, St. 5 Nihonmatsu, and St. 6 Akutsu; **Figure S1**). Samples were taken during stable water discharge periods in the summer (July, 2012 and June 2015) and winter (January, 2013) 1.5 to 4 years after the accident. The lentic area near the river bank (water depth of <20 cm) was selected as the main sampling site for deposited sediment. In St. 4 Fukushima, deposited sediments were also collected from the river bank in the flood plain. During sampling, sediments were carefully collected from the surface layer (layer depth of less than 2–3 cm) in a 100 mL polystyrene container by using a plastic scoop and a gloved hand. The sediment surface layer in the lentic areas was mostly composed of finer particles (<2 mm) compared with those present in the bottom of lotic area. Indeed, the river bed in the lotic area of most sampling

sites consisted of large particles, including gravel and stones, and fine particles were neither observed on the surface of river bed by visual inspection from river bank nor collected sufficiently with the Ekman-Birge grab sediment sampler.

During the sample collection, water samples (40–100 L) were also collected in a polypropylene container from either the river bank or top of a bridge by using plastic pump (Tempest DTW 60ft, Proactive). To investigate the origins of OM in the Abukuma River sediments, end-member samples, such as terrestrial soil, terrestrial plants, and riverine algae, were also collected along the Abukuma River basin in December 2014 and June 2015 (in the vicinity of the sediment sampling stations. The collected sediment, water, and end-member samples were transported to the experimental laboratory immediately after the completion of the field survey. While the end-member and sediment samples were collected from different multiple years, temporal trends of sample data were indiscernible among the deposited and suspended sediments as well as the end-member samples, at least, for a few years' data set investigated in this study, as discussed below.

2.2 Pretreatment of sediment samples

Sediment samples were pretreated according to the standard protocol for clay mineralogical analyses(The Clay Science Society of Japan 2009). The deposited sediments were air-dried on a ceramic plate at room temperature (25°C) for several days. The dried samples were then gently homogenized with a mortar to break up the physically aggregated particles. The fine sediment particles

149 with size less than 2 mm were collected by a fractionation using 2 mm-pore size sieve. The
150 homogenization and sieving were repeated when small aggregates were still visible. Suspended
151 sediment samples were collected by vacuum filtration of the collected river water with 1 μm
152 hydrophilic polytetrafluoroethylene (PTFE) membrane filter (47 mm, Millipore, Japan). The dried
153 suspended sediments were finally obtained by resuspending the sediments on the filter in ultrapure
154 Milli-Q water (MQ; Millipore; 18.2 MΩ·cm resistivity at 25°C) and lyophilizing the suspension with
155 a vacuum freeze dryer (FDU-1200, EYELA, Japan) overnight. The deposited and suspended sediment
156 samples were stored in a desiccator in the dark condition when not in use.
157
158 **2.3 Density separation**
159 The density fractionation of sediment particles was performed based on the method used by
160 Arnarson and Keil(Arnarson and Keil 2001) with some modifications. Sodium polytungstate (SPT;
161 $Na_6[H_2W_{12}O_{40}]$, TC-Tungsten Compounds, Germany) was used as a heavy liquid. A solution of SPT
162 with a density of 2.8 $g \cdot cm^{-3}$ in MQ water was prepared, and dried sediments were added at a sediment
163 dry weight-to-solution volume (SDW/SV) ratio of 0.5 $g \cdot mL^{-1}$. The sediment suspensions were
164 sonicated in a polypropylene container for 10 min followed by subsequent gentle agitation using a
165 shaker for 10 min to disperse aggregated particles loosely bound by cross-linkage via OM(Arnarson
166 and Keil 2001, Golchin et al. 1994). The suspension was then centrifuged for 20 min at 2,000 g at
167 room temperature. The heavier fraction pellet was resuspended in 2.8 $g \cdot cm^{-3}$ SPT, agitated and

centrifuged three times until no lighter particles were found to be suspended by visual inspection. At each step, supernatant containing the lighter fraction was carefully collected by pipette and stored for the next separation treatment. To remove SPT, the pellet (density of > 2.8 $g \cdot cm^{-3}$) was washed by resuspending in MQ and centrifuging three times. After decanting, the pellet was lyophilized by the vacuum freeze dryer and stored in a desiccator.

The supernatant in 2.8 $g \cdot cm^{-3}$ SPT was further diluted by adding MQ to adjust the SPT solution density to 2.6 $g \cdot cm^{-3}$. By repeating the aforementioned processes, 2.6–2.8 and <2.6 $g \cdot cm^{-3}$ sediment fractions were collected as a pellet and supernatant, respectively, after centrifugation. These processes were repeated for the 2.4, 2.2, 2.0, 1.8 and 1.6 $g \cdot cm^{-3}$ SPT solutions to obtain sediments with different densities. The lowest density (>1.6 $g \cdot cm^{-3}$) sediment fraction was collected by filtering the supernatant in 1.6 $g \cdot cm^{-3}$ SPT with a 1 μm PTFE membrane filter, followed by washing, resuspension in MQ and lyophilization.

2.4 Hydrogen peroxide treatment

Sediments were treated with H_2O_2 to remove the OM fraction (The Clay Science Society of Japan 2009). The dried sample was added to 8.6% H_2O_2 solution (Kanto Chemical, Japan) at a SDW/SV ratio of 0.14 $g \cdot mL^{-1}$ and initially heated at 60 °C for 10 min. After bubbling ceased, the solution was heated for 1 h at 80 °C, at which disproportionation of H_2O_2 is promoted, to remove the remaining H_2O_2. To minimize the readsorption of extracted RCs on the sediment particles, SCs (cesium

187 chloride, 133-Cs, Kanto Chemical) was added to the H_2O_2-sediment mixture at a final concentration
188 of ~200 μM. The ratio of SCs relative to SDW (SCs/SDW) was adjusted to 1.8–2.5 μmol·g^{-1}, which
189 was greater than the Cs adsorption capacity for the selected samples (e.g., 0.38–1.2 μmol·g^{-1}; see
190 **Supplementary Material SM 2** for details). In this case, almost all (>99%) the Cs adsorption sites in
191 the sediments were calculated to be occupied and SCs adsorption was expected to prevent readsorption
192 of dissociated RCs. H_2O_2 treatment was conducted at different H_2O_2 concentrations and digestion times
193 at 60 °C to examine the relationship between RCs removal with the degree of OM digestion (see
194 **Supplementary Material SM 1.10** for details).
195
196 **2.5 Other chemical treatments**
197 Some deposited sediments were treated with the dithionite-citrate, acid ammonium oxalate,
198 and acid hydroxylamine methods to remove amorphous inorganic particles(Carter and Gregorich
199 2007). These treatments dissolve non-crystalline aluminosilicates, Fe oxides, and organically
200 complexed metals, including Al, Fe, and Mn, via ligand- and reduction-promoted processes, although
201 the methods are much less effective in removing crystalline Al. The treatments were conducted by
202 using the standard protocol described elsewhere(Carter and Gregorich 2007), except that excess SCs
203 was amended in this study to the sample solution to prevent readsorption of dissociated RCs
204 (SCs/SDW of ~2.0 μmol·g^{-1} and SDW/SV of 0.14 g·mL^{-1}).
205 The dried sediments were treated at a SDW/SV ratio of ~0.75 g·mL^{-1} with 1 M HCl (Kanto

206 Chemical), 1 M HNO_3 (Kanto Chemical), 1 M NaOH (Kanto Chemical), 1 M ammonium acetate
207 (Kanto Chemical), and MQ water. Again, in all cases, the solution was amended with SCs at final
208 concentrations of ~200 μM, corresponding to SCs/SDW of 1.6–2.1 $\mu mol \cdot g^{-1}$. Sediment suspensions
209 were then incubated for an hour at 25 °C under gentle agitation. After centrifuging and decanting the
210 supernatant, the pellets were washed three times by resuspending in MQ and centrifuging. The washing
211 process was repeated for three times followed by the freeze drying.
212
213 **2.6 Sample analysis**
214 A full description of the sample analyses is provided in the **Supplementary Material (SM**
215 **1)**. Briefly, the radioactivity concentrations ($Bq \cdot g^{-1}$) of 134-Cs and 137-Cs in the treated and untreated
216 dried sediments were determined by 604 and 661 keV gamma-rays using a germanium semiconductor
217 detector (SEGEMS GEM20-70, Seiko EG&G Co., Ltd., Japan). The decay of the activity was
218 corrected to the date of accident (March 14, 2011). Organic C and N contents and N/C ratio were
219 measured by an elemental analyzer (Flash EA ConFlo III, Thermo Electron Corporation, USA)
220 equipped with an isotope ratio mass spectrometer (Delta V Advantage, Thermo Fisher Scientific, USA).
221 Specific surface area of sediment was determined by the N_2 gas adsorption method using the automatic
222 surface area and porosimetry analyzer (TriStar II 3020, Micrometritics, USA). Prior to analyzing the
223 specific surface area, the H_2O_2-treated samples were heated at 350 °C for 5 h and evacuated with a
224 vacprep degasser (VacPrep 061LB, Micromeritics) to remove pre-adsorbed gases and water vapor from

the sample. Sediment particle size was determined by laser diffraction and scattering at 690 nm (SALD 3000S, Shimadzu, Japan). X-ray diffraction analysis of an oriented specimen was performed with an X-ray diffractometer (X'pert-MPD-OEC, Philips). Microscope images of the sediment samples were obtained by SEM (VE-9800, Keyence, Japan) and optical microscopy (TC5000, Meiji Techno, Japan).

3. Results and Discussion

3.1 RCs concentrations in deposited and suspended sediments

Concentrations of RCs (defined as the sum of radioactivity for 134-Cs and 137-Cs [Bq] per unit mass of dried sediment [kg]) ranged from 659 to 31,274 $Bq \cdot kg^{-1}$ in air-dried or lyophilized samples of deposited and suspended sediments (**Table S1** and **Figure S3**). The average ratio of 134-Cs/137-Cs was determined to be 0.99 for all the samples examined in this study ($n = 87$), consistent with the ratio emitted from the FDNPP(Buesseler et al. 2011). The RCs concentrations of suspended sediment (8282–31,274 $Bq \cdot kg^{-1}$, average of 16,834 $Bq \cdot kg^{-1}$) were statistically greater than those for deposited sediment (659–10,843 $Bq \cdot kg^{-1}$, average of 4891 $Bq \cdot kg^{-1}$) according to a single-tailed heteroscedastic *t*-test ($p < 9.5 \times 10^{-5}$, $n = 9$–11) (**Figure S3**). For the sample set of suspended sediment, the RCs concentration in winter 2013 (16,397–31,274 $Bq \cdot kg^{-1}$, average of 20,500 $Bq \cdot kg^{-1}$) was higher than those collected in summer 2012 (8282–14,705 $Bq \cdot kg^{-1}$, average of 12,253 $Bq \cdot kg^{-1}$, $p < 0.029$, $n = 4$–5), though these winter and summer samples were taken in different years. Spatial and seasonal trends in RCs concentration were statistically indiscernible when deposited and suspended sediments were

pooled, even though the RCs deposition in the terrestrial environment varies substantially in the Abukuma River catchment (**Figure S1**). Such a spatiotemporal variation in sedimentary RCs in rivers may be reasonable, given that riverine sediments are a mixture of particles from a range of terrestrial and aqueous sources in the catchment(Sakaguchi et al. 2015). Nonetheless, long-term monitoring with higher sampling frequency would be important to understand the spatiotemporal mobility of RCs in the riverine sediments and other aqueous environments in the catchment.

As a preliminary test to extract the factors relevant to sedimentary RCs concentration, a simple correlation analysis was performed on RCs concentration and sediment properties, including organic C and N content (%, defined as the mass of C or N per unit mass of dried sediment), N/C ratio, specific surface area ($m^2 \cdot g^{-1}$), and sediment particle size (μm). The Pearson's (R) correlation coefficients were determined for all samples in addition to the subset of samples collected in 2012, 2013, and 2015 (**Table S1**). Statistically significant correlations were observed for some parameters associated with OM except for the sample set for 2015. For example, C and N contents showed the highest positive correlations with RCs concentration ($p < 0.01$, R and ρ 0.69–0.72 for all samples, **Figures 1a and 1b**), and suspended sediment had higher C and N contents compared with deposited sediment. In addition, specific surface area determined by the N_2 adsorption BET method showed a significant correlation with RCs concentration **(Figure 1c)**. In addition, the specific surface area had a positive correlation with organic C content **(Figure 1d)**. In contrast to the specific surface area, neither sediment size nor surface area determined by the laser diffraction/scattering method had a significant correlation with

sedimentary RCs concentration **(Figures 1e and 1f)**.

3.2 RCs distribution in density-separated sediments

Sediment fractions with a wide spectrum of OM contents (0.15–24%, **Table S2**) were obtained by separating deposited sediment samples collected at three sampling stations (St. 1 Watari, St. 2 Marumori, and St. 4 Fukushima) into eight fractions with the density-based method. Hereafter, sample fractions with densities of >2.4, 1.8–2.4, and <1.8 $g \cdot cm^{-3}$ are referred to as heavy, intermediate, and light fractions, respectively. The organic C measurement undoubtedly indicated gradual increase in OM content with decreasing sediment density **(Table S2)**. The scanning electron microscopy (SEM) images demonstrated a gradient in the fractionated sediment morphology from crystalline particles for heavy fractions to amorphous aggregate for light fractions (**Figure S4**). The X-ray diffraction (XRD) analysis were consistent with the SEM observations. Distinct peaks corresponding to the crystalline structure of clay minerals, such as mica and amphibole that appear in the lower angle region (<10°), were found for the heavy fractions, whereas such peaks became indiscernible for the intermediate and light fractions **(Figure S5)**. The peaks associated with quartz also decreased with decreasing density and only a few small peaks were seen for the light fractions, indicating the dominance of the amorphous structure in the light fractions.

For the deposited sediments, the RCs concentrations in the light and intermediate fractions (1527–19,288 $Bq \cdot kg^{-1}$, $n = 24$) were greater than those in the heavy fractions (148–8150 $Bq \cdot kg^{-1}$, $n =$

8) at a statistically significant level ($p < 2.4 \times 10^{-3}$ according to a single-tailed heteroscedastic *t*-test) **(Figure S6a)**. The deposited sediments from St. 1 Watari in 2012 and St. 4 Fukushima in 2015 had the highest RCs concentrations in the lowest density fraction (<1.6 g·cm^{-3}, 17,123–19,288 Bq·kg^{-1}), whereas the highest RCs concentrations were found in fractions with densities of 1.6–1.8 g·cm^{-3} (14,356 Bq·kg^{-1}) and 2.0–2.2 g·cm^{-3} (12,105 Bq·kg^{-1}) for the sediments from St. 2 Marumori and St. 4 Fukushima in 2013, respectively. The RCs concentrations for the light fraction were larger than those for the parent unseparated sediment samples. For the suspended sediments, the highest RCs concentrations were also observed in the light and intermediate fractions (<2.4 g·cm^{-3}) for the all sampling stations examined (**Figure S7a)**. In contrast to the RCs concentrations, the proportion of RCs activity in each fraction (%, defined as the ratio of RCs activity for each fraction [Bq] relative to the sum of RCs activity for all fractions [Bq]) was always highest in the intermediate fractions because the majority of sediment weight was accounted for by the density fractions of 1.8–2.4 g·cm^{-3} **(Figures S6b, S6c, S7b and S7c)**.

For the density-separated sediment, the RCs concentration was positively correlated with organic C content **(Figure 2**), consistent with the results for the unseparated sediments. In particular, heavy and intermediate fractions with a C content less than 6% showed a linear relationship (R=0.90, p=1.6 x 10^{-9}, n=24, **Figure 2a**). In contrast, for the light fractions with a high organic C content (>7%), the RCs concentrations were relatively constant or even dropped as the organic C content increased. Thus, correlation between RCs and organic C contents became relatively week when all data were

301 pooled (i.e., R=0.61, p=2.0 x 10^{-4}, n=32). Likewise, RCs concentrations for suspended sediment
302 substantially fluctuated at higher organic C contents (R=0.61, p=0.10, n=8, **Figure 2b**). Visual
303 inspection with an optical microscope indicated that the lightest fraction with lower RCs
304 concentrations (i.e., outlier data) contained relatively large amount of large-size terrestrial OM, such
305 as wood debris and leaves, in contrast to the heavy and intermediate fractions which mainly contained
306 fine particles (**Figures 3** and **S8**). This microscopic observation invokes the notion that lower RCs
307 concentrations arose from the smaller surface area. Indeed, the positive correlations were also found
308 for RCs versus specific surface area as well as organic C content versus specific surface area for the
309 density-separated samples (**Figures 2c and 2d**). The former plot demonstrated positive linear
310 relationship with no outlier data for the samples examined, which is further discussed in detail as noted
311 below.
312
313 **3.3 Source of sedimentary OM**
314 The N/C ratio was analyzed to investigate the source of OM present in sediment samples. The
315 parameters were compared with those for the end-member samples collected along the Abukuma River
316 basin (e.g., terrestrial plants, soil OM, and riverine microalgae [periphyton]; **Table S3**). The end-
317 member samples were selected according to the land use coverage in the Abukuma River catchment
318 (**Figure S1)**.
319 The N/C ratios for the riverine and terrestrial OM showed distinct variation ($p < 0.05$; Tukey's

test; **Figure 4**). For example, N/C for riverine algae (0.10–0.14) was higher than for terrestrial plants and soil OM (0.01–0.09), which consist of OM with low N/C ratios such as lignin and cellulose(Sato et al. 2006). The ranges for these end-members samples were consistent with previous reports for terrestrial C_3 higher plants (less than ~0.05)(Hedges et al. 1986) and phytoplankton (0.09–0.2)(Finkel et al. 2010). The N/C ratios for unseparated suspended and deposited sediments (0.09–0.14) were comparable to those for riverine algae. Although some of the deposited sediments showed lower N/C ratios (0.07–0.14) than those for the suspended sediments, the N/C ratios for deposited sediments were still statistically higher than those for the terrestrial plants and soil OM ($p < 0.05$; Tukey's test).

In the density-separated samples, N/C ratios for the heavy and intermediate fractions (0.07–0.13) were comparable to suspended sediment and riverine algae. In contrast, light fractions showed lower N/C ratios (0.04–0.09), which were similar to the N/C ratios for terrestrially derived soil OM (0.04–0.09). It should be noted that terrestrial plant has a relatively lower N/C ratio due to the presence of carbon rich components such as lignin and cellulose (Hedges et al. 1986). these results suggested that OM present in the light density fractions is mainly accounted for by allochthonous OM (i.e., terrestrial origin), whereas the intermediate fractions likely contained autochthonous OM at relatively higher proportion.

3.4 Effects of chemical treatments on radioactive Cs removal

To examine the role of OM in RCs accumulation, the unseparated deposited sediment samples

were further subjected to a range of chemical treatments. The H_2O_2 treatment removed substantial portion of sedimentary OM (e.g., 60–86% and 65–77% of organic C and N, respectively) (**Figure S9**). Consistently, the SEM images demonstrated the removal of amorphous aggregates after the H_2O_2 treatment (**Figure S4**). In contrast to OM removal, the residual rates of RCs, defined as the ratio of residual RCs concentration after treatment to initial RCs concentration, were greater than 0.60 with an average ± standard deviation of 1.0 ± 0.20 for the samples examined (n = 12, **Figure S9** and **Table S4**). This result indicated that RCs concentrations were stable against to H_2O_2-assisted OM digestion.

We speculated that a significant amount of RCs had been released into the water column during the H_2O_2 digestion: yet, most of the RCs was detected in the particulate fraction owing to readsorption onto the sediment surface. Therefore, we conducted the H_2O_2 treatment using a solution amended with a high concentration of stable Cs (SCs; 133-Cs) to mask the sites potentially available for readsorption of dissociated RCs. The ratio of SCs to sediment dry weight was adjusted to values greater than the Cs adsorption capacity per unit mass of sediment (see **Supplementary Material SM 2** for details). However, the observed insignificant removal of RCs in the presence of excess SCs (**Figure S9**) suggests that the dissociation of RCs from the sediment particles to the water column was negligible during the digestion treatment. Thus, our data indicates that little RCs was accumulated in or directly associated with the organic compounds in the sediments examined, unless otherwise RCs was specifically and locally accumulated in the fraction of H_2O_2-recalcitrant OM, such as pyrogenic materials, aliphatic compounds, or other organic constituents like lignin-derived and N-containing

compounds(Mikutta et al. 2005). Nonetheless, the modified H_2O_2 treatments yielding higher removal rates of OM (up to 96%) also resulted in insignificant reduction of RCs (**Supplementary Material SM 1.10**), indicating that the accumulation of RCs in refractory organic compounds is less likely.

To investigate the nature of sedimentary RCs further, we conducted treatments using various chemicals such as strong acid (HNO_3 and HCl), alkaline (NaOH) and ammonium acetate solutions in addition to digestion of non-crystalline minerals using dithionite-citrate, acid ammonium oxalate and acid hydroxylamine methods **(Figure S10)**. However, all the treatments resulted in either a negligible or small reduction of RCs concentration (residual rates greater than 0.70). Given that soil OM has been reported to be highly stabilized by non-crystalline minerals(Torn et al. 1997), amorphous inorganic and organic mixtures were also suspected to be the candidates of RCs carriers. However, little RCs was extracted by the dithionite-citrate, acid ammonium oxalate, and acid hydroxylamine methods, which are capable of extracting organically complexed metals (Al, Fe, Mn), amorphous inorganic Al, Fe and Mn forms and non-crystalline aluminosilicates (e.g., allophane and imogolite)(Carter and Gregorich 2007). Note that these methods are less effective in removing crystalline oxides and hydroxides of Al and virtually no metals from crystalline silicate minerals(Carter and Gregorich 2007). The results generally suggested that the RCs present in our sediments is chemically non-labile and perhaps fixed by micaceous or other clay minerals in a relatively stable manner.

3.5 Correlation of RCs and sediment specific surface area

377 The apparent correlation of RCs and OM contents is likely attributed to the relationship
378 between OM and specific surface area. Our data indicated that the organic C content is significantly
379 and positively correlated with the specific surface area for the unseparated and density-fractionated
380 sediments **(Figures 1d and 2d)**. The previous findings also indicated that the OM content are highly
381 correlated with particle surface area determined by gas adsorption in the majority of soils and river
382 and coastal sediments(Bergamaschi et al. 1997, Keil et al. 1997, Mayer 1994, 1999). In addition, the
383 particulate organic C-to-surface area ratios (OC/SA) for our unseparated samples (0.24–1.4 mg-C·m^2)
384 were comparable to those determined for river sediments in previous work (0.43–0.91 mg-C·m^2) (Keil
385 et al. 1997).
386 The OC/SA (36.6 mg-C·m^2) for the density-separated outlier sample with a low RCs
387 concentration at high organic C content was an order of magnitude greater than the unseparated
388 samples, indicating extremely low surface area per unit mass of organic C most likely due to the
389 significant participation of large-size allochthonous OM (e.g., woody debris or leaf fragments; **Figure**
390 **3**). In such case, RCs concentration did not necessarily increase with increasing OM content, which is
391 in contrast to the positive correlation between specific surface area and RCs concentration for the all
392 samples **(Figure 5)**. The linear relationship between RCs concentration and specific surface area
393 suggests that RCs carrying capacity per unit of sediment surface area is relatively constant and
394 irrespective of OM source. The adsorption process of RCs and clay minerals (e.g., illite and biotite)
395 are well documented in literature and the RCs adsorption is in many cases related to the particle size

396 and surface area of sediment (e.g., Mukai et al., 2014; Yoshimura et al., 2014). Mukai et al. (2014), for
397 example, reported that RCs adsorption to the finer biotite was greater for the RCs-contaminated soil
398 particles in Fukushima indicating the importance of surface are of minerals to the RCs adsorption.
399 Because the majority of RCs activity in sediment occurred in the intermediate density
400 fractions (1.8–2.4 $g \cdot cm^{-3}$, **Figures S6 and S7**), where OM is mainly characterized by autochthonous
401 origin (according to the N/C ratio analysis), the RCs concentration in the riverine deposited and
402 suspended sediments is mostly related with the autochthonous OM. The monolayer hypothesis
403 proposes that sedimentary OM does not equally cover the particle surface. Rather, OM occurs in a
404 patch manner(Mayer 1999) and play important role in cross-linkage of organic and mineral
405 aggregates(Bock and Mayer 2000). As noted below in more detail, such role of autochthonous OM is
406 likely important in the accumulation of the RCs-contaminated inorganic mineral particles in riverine
407 sediments. A previous study also indicated that most fluvial particulate OM is closely associated with
408 suspended minerals(Keil et al. 1997), though some portions of particulate OM may occur as discrete
409 large-size organic particles (fragments) with this type of OM most likely to be allochthonous
410 origin(Keil et al. 1997).In contrast to the specific surface area, the particle diameter and surface area
411 determined by the laser scattering technique did not have a significant relationship with RCs or OM
412 (**Table S1**). In addition, the surface area calculated with this technique was smaller than the BET
413 specific surface area by one or two orders of magnitude. The lack of significant correlation suggests
414 that the laser scattering technique is insufficient to quantify, with high accuracy, the microstructure of

fine particulate surface including RCs fixing and adsorption sites.

3.6 Potential mechanism behind the correlation of RCs and autochthonous OM

Given the chemically inert nature of sedimentary RCs observed in this and previous studies, the results from this study indicate that RCs in riverine sediment is fixed by the clay minerals (e.g., biotite) most likely via irreversible process (Mukai et al., 2014). While aqueous and sedimentary fine particles are generally composed of various components such as organisms (e.g., phytoplankton, terrestrial plant fragments, other organisms), detritus (e.g, fecal pellet) and inorganic matters, fine clay minerals can form microaggregates with autochthonous OM including phytoplankton (Alldredge and Silver, 1988; De La Rocha et al., 2008). However, it should be noted that previous studies consistently indicated that direct association of mineral particles and phytoplankton is unlikely (Ransom et al.,1999). Rather, extracellular polymeric substances such as polysaccharides are recognized to play a role in the formation of organic and inorganic miroaggregates. Such polymeric substances are most likely secreted by surrounding microorganisms such as bacteria and phytoplankton and contribute to the stabilization of organic and inorganic aggregates via cation-mediated cross-linkage (Verdugo et al., 2004; Hamm 2002; Kovac et al., 2014; Deng et al., 2015). Therefore, it is likely that such polymeric substances acted as a glue of clay minerals and autochthonous OM forming the microaggregates in our riverine fine sediments.

Given that microorganisms and polymeric organic substances preferentially sequesters the

434 fine particles with high surface area (primarily clay minerals) in marine sediments (Ransom et al.,
435 1998), specific surface area of sediment is more likely controlled by the fine inorganic particles rather
436 than organic matters. It would be reasonable, therefore, to conclude that the observed correlations
437 among RCs, autochthonous OM and specific surface area of sediment is due to the accumulation of
438 RCs-contaminated fine minerals in the OM-rich sediment. Indeed, in the specific surface area analysis,
439 we removed sedimentary organic matters prior to the BET measurement via combustion treatment, as
440 such the BET measurement in this study represents the surface area of inorganic fraction of sediment.
441 It has been well recognized that soil OM such as humic substances can adsorb onto the surface
442 of clay minerals and such soil OM exerts a hindering effect on Cs adsorption to clay minerals via
443 covering or blocking the specific adsorption site (e.g., FES). Thus, Cs mobility and bioavailability are
444 enhanced in the presence of soil OM (Staunton et al., 2002). However, possible differences in the role
445 of soil and aqueous OM in terms of RCs interaction is, at least partially, related to timing of Cs
446 adsorption to clay minerals during the longitudinal transport from terrestrial runoff to downstream
447 river systems. In contrast to soil OM, interaction of autochthonous OM with RCs in aqueous sediment
448 occurs in the river systems. In such case, RCs is already carried by the fine minerals, and dissolution
449 of RCs from minerals to aqueous phase and subsequent steric hindrance of aqueous RCs re-adsorption
450 to minerals by autochthonous OM are less likely to occur simply because of the irreversible nature of
451 RCs fixation to the minerals.
452

4. Conclusions

The present study investigated the characteristics of fine sediments and FDNPP-derived RCs in the Abukuma River, Japan with emphasis on the association of RCs with sedimentary OM. Comprehensive analyses of the RCs concentration and physicochemical properties of sediments indicated strong relationship between RCs concentration and OM contents for the suspended and deposited sediments and the density-separated samples. In particular, the significant correlation between OM and RCs was observed for the intermediate density sediments where the highest proportion of RCs activity was found and autochthonous OM dominantly occurs. The correlation did not hold for some light density fractions due to the presence of large-size allochthonous OM.

Despite the correlation of RCs concentration and OM content, removing the majority of sedimentary OM by H_2O_2 treatment resulted in the small reduction of RCs concentration, indicating that the direct association of RCs with sedimentary OM is less likely. The BET specific surface area was correlated with sedimentary RCs concentration, and this variable could explain the outlier sample, which showed relatively low RCs concentration at high OM content. These results combined with the fact that sedimentary RCs was not extractable in a series of chemical digestion assays indicated that finer-grained and chemically non-labile inorganic minerals associated with autochthonous OM are an important carrier of RCs.

The lower chemical reactivity of RCs in riverine sediment is consistent with the short biological decay of grazing fish (e.g., *Plecoglossus altivelis*) in the Abukuma River after the FDNPP

accident (half-life of ~39 days)(Iguchi et al. 2013). Given that the major pathway of RCs contamination in such grazing fish species is via intake of autochthonous OM, the short retention time of RCs is at least partially associated with the lower digestibility of the contaminated inorganic sediment in the fish body. Furthermore, the longer decay of RCs for fish species in freshwater lakes with longer hydraulic time may be relevant to the greater autochthonous OM production and RCs retention in ecosystems after the FDNPP accident(Fukushima and Arai 2014). Finally, autochthonous OM in the water bodies can be an important carrier and sink for terrestrially derived RCs-contaminated soil particles. This notion, for example, implies that algal pond may be useful for the remediation of contaminated aqueous environment and higher priority for decontamination may be given to the fine sediment in lentic areas where autochthonous OM dominates. Therefore, autochthonous OM is of great concern in view of the mobility, bioavailability, and fate of FDNPP-derived RCs in aqueous and sedimentary environments.

Acknowledgements

This study is supported by JSPS Grant-in-Aid for Scientific Research (15 H 00972). In addition, analyses of SEM and X-ray diffraction were supported by Ookayama Materials Analysis Division Technical Department in Tokyo Institute of Technology.

488 **References**

489 Alldredge, A.L. and Silver, M.W. (1988) Characteristics, Dynamics and Significance of Marine Snow.
490 Progress in Oceanography 20(1), 41-82.

491 Ambe, D., Kaeriyama, H., Shigenobu, Y., Fujimoto, K., Ono, T., Sawada, H., Saito, H., Miki, S., Setou,
492 T., Morita, T. and Watanabe, T. (2014) Five-minute resolved spatial distribution of radiocesium in sea
493 sediment derived from the Fukushima Dai-ichi Nuclear Power Plant. Journal of Environmental
494 Radioactivity 138, 264-275.

495 Arnarson, T.S. and Keil, R.G. (2001) Organic-mineral interactions in marine sediments studied using
496 density fractionation and X-ray photoelectron spectroscopy. Organic Geochemistry 32(12), 1401-1415.

497 Bergamaschi, B.A., Tsamakis, E., Keil, R.G., Eglinton, T.I., Montlucon, D.B. and Hedges, J.I. (1997)
498 The effect of grain size and surface area on organic matter, lignin and carbohydrate concentration, and
499 molecular compositions in Peru Margin sediments. Geochimica Et Cosmochimica Acta 61(6), 1247-
500 1260.

501 Bock, M.J. and Mayer, L.M. (2000) Mesodensity organo-clay associations in a near-shore sediment.
502 Marine Geology 163(1-4), 65-75.

503 Bostick, B.C., Vairavamurthy, M.A., Karthikeyan, K.G. and Chorover, J. (2002) Cesium adsorption on
504 clay minerals: an EXAFS spectroscopic investigation. Environmental Science & Technology 36(12),
505 2670-2676.

506 Buesseler, K., Aoyama, M. and Fukasawa, M. (2011) Impacts of the Fukushima nuclear power plants
507 on marine radioactivity. Environmental Science & Technology 45(23), 9931-9935.

508 Carter, M.R. and Gregorich, E.G. (2007) Soil Sampling and Methods of Analysis, Second Edition,
509 CRC Press, Florida.

510 Comans, R.N.J., Haller, M. and Depreter, P. (1991) Sorption of Cesium on Illite - Nonequilibrium
511 Behavior and Reversibility. Geochimica Et Cosmochimica Acta 55(2), 433-440.

512 Comans, R.N.J. and Hockley, D.E. (1992) Kinetics of Cesium Sorption on Illite. Geochimica Et
513 Cosmochimica Acta 56(3), 1157-1164.

514 Cornell, R.M. (1993) Adsorption of Cesium on Minerals - a Review. Journal of Radioanalytical and

515 Nuclear Chemistry-Articles 171(2), 483-500.

516 De La Rocha, C.L., Nowald, N. and Passow, U. (2008) Interactions between diatom aggregates,
517 minerals, particulate organic carbon, and dissolved organic matter: Further implications for the ballast
518 hypothesis. Global Biogeochemical Cycles 22(4).

519 Deng, W., Monks, L. and Neuer, S. (2015) Effects of clay minerals on the aggregation and subsequent
520 settling of marine Synechococcus. Limnology and Oceanography 60(3), 805-816.

521 Fan, Q.H., Tanaka, M., Tanaka, K., Sakaguchi, A. and Takahashi, Y. (2014) An EXAFS study on the
522 effects of natural organic matter and the expandability of clay minerals on cesium adsorption and
523 mobility. Geochimica Et Cosmochimica Acta 135, 49-65.

524 Finkel, Z.V., Beardall, J., Flynn, K.J., Quigg, A., Rees, T.A.V. and Raven, J.A. (2010) Phytoplankton
525 in a changing world: cell size and elemental stoichiometry. Journal of Plankton Research 32(1), 119-
526 137.

527 Fukushima, T. and Arai, H. (2014) Radiocesium contamination of lake sediments and fish following
528 the Fukushima nuclear accident and their partition coefficient. Inland Waters 4(2), 204-214.

529 Golchin, A., Oades, J.M., Skjemstad, J.O. and Clarke, P. (1994) Soil-Structure and Carbon Cycling.
530 Australian Journal of Soil Research 32(5), 1043-1068.

531 Hamm, C.E. (2002) Interactive aggregation and sedimentation of diatoms and clay-sized lithogenic
532 material. Limnology and Oceanography 47(6), 1790-1795.

533 He, Q. and Walling, D.E. (1996) Interpreting particle size effects in the adsorption of Cs-137 and
534 unsupported Pb-210 by mineral soils and sediments. Journal of Environmental Radioactivity 30(2),
535 117-137.

536 Hedges, J.I., Clark, W.A., Quay, P.D., Richey, J.E., Devol, A.H. and Santos, U.D. (1986) Compositions
537 and Fluxes of Particulate Organic Material in the Amazon River. Limnology and Oceanography 31(4),
538 717-738.

539 Hedges, J.I. and Keil, R.G. (1995) Sedimentary Organic-Matter Preservation - an Assessment and
540 Speculative Synthesis. Marine Chemistry 49(2-3), 81-115.

541 Iguchi, K., Fujimoto, K., Kaeriyama, H., Tomiya, A., Enomoto, M., Abe, S. and Ishida, T. (2013)

542 Cesium-137 discharge into the freshwater fishery ground of grazing fish, ayu Plecoglossus altivelis
543 after the March 2011 Fukushima nuclear accident. Fisheries Science 79(6), 983-988.

544 Keil, R.G., Mayer, L.M., Quay, P.D., Richey, J.E. and Hedges, J.I. (1997) Loss of organic matter from
545 riverine particles in deltas. Geochimica Et Cosmochimica Acta 61(7), 1507-1511.

546 Kim, Y., Cygan, R.T. and Kirkpatrick, R.J. (1996a) Cs-133 NMR and XPS investigation of cesium
547 adsorbed on clay minerals and related phases. Geochimica Et Cosmochimica Acta 60(6), 1041-1052.

548 Kim, Y., Kim, K., Kang, H.D., Kim, W., Doh, S.H., Kim, D.S. and Kim, B.K. (2007) The accumulation
549 of radiocesium in coarse marine sediment: Effects of mineralogy and organic matter. Marine Pollution
550 Bulletin 54(9), 1341-1350.

551 Kim, Y., Kirkpatrick, R.J. and Cygan, R.T. (1996b) Cs-133 NMR study of cesium on the surfaces of
552 kaolinite and illite. Geochimica Et Cosmochimica Acta 60(21), 4059-4074.

553 Kinoshita, N., Sueki, K., Sasa, K., Kitagawa, J., Ikarashi, S., Nishimura, T., Wong, Y.S., Satou, Y.,
554 Handa, K., Takahashi, T., Sato, M. and Yamagata, T. (2011) Assessment of individual radionuclide
555 distributions from the Fukushima nuclear accident covering central-east Japan. Proceedings of the
556 National Academy of Sciences of the United States of America 108(49), 19526-19529.

557 Koarashi, J., Atarashi-Andoh, M., Matsunaga, T., Sato, T., Nagao, S. and Nagai, H. (2012) Factors
558 affecting vertical distribution of Fukushima accident-derived radiocesium in soil under different land-
559 use conditions. Science of the Total Environment 431, 392-401.

560 Kogure, T., Morimoto, K., Tamura, K., Sato, H. and Yamagishi, A. (2012) XRD and HRTEM Evidence
561 for Fixation of Cesium Ions in Vermiculite Clay. Chemistry Letters 41(4), 380-382.

562 Kovac, N., Faganeli, J., Bajt, O., Sket, B., Orel, B. and Penna, N. (2004) Chemical composition of
563 macroaggregates in the northern Adriatic sea. Organic Geochemistry 35(10), 1095-1104.

564 Kusakabe, M., Oikawa, S., Takata, H. and Misonoo, J. (2013) Spatiotemporal distributions of
565 Fukushima-derived radionuclides in nearby marine surface sediments. Biogeosciences 10(7), 5019-
566 5030.

567 Lepage, H., Evrard, O., Onda, Y., Lefevre, I., Laceby, J.P. and Ayrault, S. (2015) Depth distribution of
568 cesium-137 in paddy fields across the Fukushima pollution plume in 2013. Journal of Environmental
569 Radioactivity 147, 157-164.

570 Matsuda, N., Mikami, S., Shimoura, S., Takahashi, J., Nakano, M., Shimada, K., Uno, K., Hagiwara,
571 S. and Saito, K. (2015) Depth profiles of radioactive cesium in soil using a scraper plate over a wide
572 area surrounding the Fukushima Dai-ichi Nuclear Power Plant, Japan. Journal of Environmental
573 Radioactivity 139, 427-434.

574 Mayer, L.M. (1994) Relationships between Mineral Surfaces and Organic-Carbon Concentrations in
575 Soils and Sediments. Chemical Geology 114(3-4), 347-363.

576 Mayer, L.M. (1999) Extent of coverage of mineral surfaces by organic matter in marine sediments.
577 Geochimica Et Cosmochimica Acta 63(2), 207-215.

578 Mikutta, R., Kleber, M., Kaiser, K. and Jahn, R. (2005) Review: Organic matter removal from soils
579 using hydrogen peroxide, sodium hypochlorite, and disodium peroxodisulfate. Soil Science Society of
580 America Journal 69(1), 120-135.

581 Mizuno, T. and Kubo, H. (2013) Overview of active cesium contamination of freshwater fish in
582 Fukushima and Eastern Japan. Scientific Reports 3.

583 Mukai, H., Hatta, T., Kitazawa, H., Yamada, H., Yaita, T. and Kogure, T. (2014) Speciation of
584 Radioactive Soil Particles in the Fukushima Contaminated Area by IP Autoradiography and
585 Microanalyses. Environmental Science & Technology 48(22), 13053-13059.

586 Mukai, H., Hirose, A., Motai, S., Kikuchi, R., Tanoi, K., Nakanishi, T.M., Yaita, T. and Kogure, T.
587 (2016) Cesium adsorption/desorption behavior of clay minerals considering actual contamination
588 conditions in Fukushima. Scientific Reports 6.

589 Murakami, M., Ohte, N., Suzuki, T., Ishii, N., Igarashi, Y. and Tanoi, K. (2014) Biological proliferation
590 of cesium-137 through the detrital food chain in a forest ecosystem in Japan. Scientific Reports 4.

591 Nagao, S., Kanamori, M., Ochiai, S., Tomihara, S., Fukushi, K. and Yamamoto, M. (2013) Export of
592 (134) Cs and (137) Cs in the Fukushima river systems at heavy rains by Typhoon Roke in September
593 2011. Biogeosciences 10(10), 6215-6223.

594 Nakai, W., Okada, N., Ohashi, S. and Tanaka, A. (2015) Evaluation of Cs-137 accumulation by
595 mushrooms and trees based on the aggregated transfer factor. Journal of Radioanalytical and Nuclear
596 Chemistry 303(3), 2379-2389.

597 Naulier, M., Eyrolle-Boyer, F., Boyer, P., Metivier, J.M. and Onda, Y. (2017) Particulate organic matter

598 in rivers of Fukushima: An unexpected carrier phase for radiocesiums. The Science of the total
599 environment 579, 1560-1571.

600 Nuclear Emergency Response Headquarters Government of Japan (2011) Additional Report of the
601 Japanese Government to the IAEA - The Accident at TEPCO's Fukushima Nuclear Power Stations-.

602 Ono, T., Ambe, D., Kaeriyama, H., Shigenobu, Y., Fujimoto, K., Sogame, K., Nishiura, N., Fujikawa,
603 T., Moritai, T. and Watanabe, T. (2015) Concentration of Cs-134+Cs-137 bonded to the organic fraction
604 of sediments offshore Fukushima, Japan. Geochemical Journal 49(2), 219-227.

605 Ransom, B., Bennett, R.H., Baerwald, R., Hulbert, V.H. and Burkett, P.J. (1999) In situ conditions and
606 interactions between microbes and minerals in fine-grained marine sediments: A TEM microfabric
607 perspective. American Mineralogist 84(1-2), 183-192.

608 Sakaguchi, A., Tanaka, K., Iwatani, H., Chiga, H., Fan, Q.H., Onda, Y. and Takahashi, Y. (2015) Size
609 distribution studies of Cs-137 in river water in the Abukuma Riverine system following the Fukushima
610 Dai-ichi Nuclear Power Plant accident. Journal of Environmental Radioactivity 139, 379-389.

611 Sato, T., Miyajima, T., Ogawa, H., Umezawa, Y. and Koike, I. (2006) Temporal variability of stable
612 carbon and nitrogen isotopic composition of size-fractionated particulate organic matter in the
613 hypertrophic Sumida River Estuary of Tokyo Bay, Japan. Estuarine Coastal and Shelf Science 68(1-
614 2), 245-258.

615 Sawhney, B.L. (1966) Kinetics of Cesium Sorption by Clay Minerals. Soil Science Society of America
616 Proceedings 30(5), 565-&.

617 Staunton, S., Dumat, C., Zsolnayc, A. (2002) Possible role of organic matter in radiocaesium
618 adsorption in soils, Journal of Environmental Radioactivity 58(2–3), 163-173.

619 Steinhauser, G., Schauer, V. and Shozugawa, K. (2013) Concentration of Strontium-90 at Selected Hot
620 Spots in Japan. Plos One 8(3).

621 Tanaka, K., Iwatani, H., Sakaguchi, A., Fan, Q.H. and Takahashi, Y. (2015) Size-dependent distribution
622 of radiocesium in riverbed sediments and its relevance to the migration of radiocesium in river systems
623 after the Fukushima Daiichi Nuclear Power Plant accident. Journal of Environmental Radioactivity
624 139, 390-397.

625 The Clay Science Society of Japan (2009) Handbook of clays and clay minerals, 3rd edition, Gihodo

(in Japanese), Tokyo.

Torn, M.S., Trumbore, S.E., Chadwick, O.A., Vitousek, P.M. and Hendricks, D.M. (1997) Mineral control of soil organic carbon storage and turnover. Nature 389, 170-173.

Verdugo, P., Alldredge, A.L., Azam, F., Kirchman, D.L., Passow, U. and Santschi, P.H. (2004) The oceanic gel phase: a bridge in the DOM-POM continuum. Marine Chemistry 92(1-4), 67-85.

Wei, L., Kinouchi, T., Yoshimura, K. and Velleux, M.L. (2017a) Modeling watershed-scale 137Cs transport in a forested catchment affected by the Fukushima Dai-ichi Nuclear Power Plant accident. Journal of Environmental Radioactivity 171, 21-33.

Wei, L.Z., Kinouchi, T., Yoshimura, K. and Velleux, M.L. (2017b) Modeling watershed-scale Cs-137 transport in a forested catchment affected by the Fukushima Dai-ichi Nuclear Power Plant accident. Journal of Environmental Radioactivity 171, 21-33.

Yamaguchi, N., Takata, Y., Hayashi, K., Ishikawa, S., Kuramata, M., Eguchi, S., Yoshikawa, S., Sakaguchi, A., Asada, K., Wagai, R., Makino, T., Akahane, I. and Hiradate, S. (2012) Behavior of radiocaesium in soil‐plant systems and its controlling factor: A review. Bulletin of the National Institute of Agro-Environmental Sciences 31, 75-129.

Yamashiki, Y., Onda, Y., Smith, H.G., Blake, W.H., Wakahara, T., Igarashi, Y., Matsuura, Y. and Yoshimura, K. (2014) Initial flux of sediment-associated radiocesium to the ocean from the largest river impacted by Fukushima Daiichi Nuclear Power Plant. Scientific Reports 4.

Yasunari, T.J., Stohl, A., Hayano, R.S., Burkhart, J.F., Eckhardt, S. and Yasunari, T. (2011) Cesium-137 deposition and contamination of Japanese soils due to the Fukushima nuclear accident. Proceedings of the National Academy of Sciences of the United States of America 108(49), 19530-19534.

Yoshimura, K., Onda, Y. and Fukushima, T. (2014) Sediment particle size and initial radiocesium accumulation in ponds following the Fukushima DNPP accident. Scientific Reports 4.

653 **Figure Captions**

654

655 **Figure 1.** Relationships among RCs concentration and parameters related to sediment quality for
656 unseparated samples: (a) RCs concentration and organic C content, (b) RCs concentration and organic
657 N content, (c) RCs concentration and specific surface area (determined by the N_2 adsorption method),
658 (d) organic C content and specific surface area (determined by the N_2 adsorption method), (e) RCs
659 concentration and particle diameter (median value determined by the laser diffraction and scattering
660 method) and (f) RCs concentration and surface area calculated from particle diameter. The data and
661 error bars represent average and standard deviation from the measurement. Regarding the symbols,
662 DS and SS represent deposited and suspended sediments and the numbers 2012, 2013 and 2015
663 indicate the sampling year. Linear regression line (solid line) and 95% confidence interval (dashed
664 line) are shown when the regression analysis is statistically significant ($p < 0.05$). Detailed values for
665 the data used in **Figure 1** are listed in **Table S1**.

666

667 **Figure 2.** Relationships among RCs concentration and sediment qualities for the density-separated
668 sediments. (a) RCs and organic C content for deposited sediment (DS: St. 1 Watari in 2012, St. 2
669 Marumori in 2013, St. 4 Fukuhima in 2013 and 2015), (b) RCs and organic C content for suspended
670 sediment (SS: St. 1 Watari in 2012, St. 2 Marumori in 2013 and St. 4 Fukushima in 2013), (c) RCs and
671 specific surface area for deposited sediment (St. 2 Marumori in 2013) and (d) organic carbon C and
672 specific surface area for deposited sediment (St. 2 Marumori in 2013). In the panels (a) an (b), data for
673 each density fraction is shown using different type of symbol. Data for the unseparated deposited
674 sediment samples were plotted together in the panels (c) and (d). The data and error bars represent
675 average and standard deviation from the measurement. Linear regression line (solid line) and 95%
676 confidence interval (dashed line) are shown in the panels (c) and (d). In the panel (d), outlier data (light
677 fraction) is shown in the bracket. Detailed values for the data used in **Figure 2** are listed in **Tables S1**
678 **and S2**.

679

680 **Figure 3.** Images from optical microscopic observation for four types of density separated deposited
681 sediment collected at St. 2 Marumori in 2013 (a_2: < 1.6 g/cm^3, b_1: 1.6-1.8 g/cm^3, d_1 : 2.0-2.2 g/cm^3 and
682 g_1 : 2.6-2.8 g/cm^3. The arrows in the right bottom figure (plot of RCs versus organic C content)
683 represent the samples a_2, b_1, d_1 and g_1 with sample a_2 being considered as outlier. Microscopic images
684 for the density separated sediment collected from other sampling stations are also shown in the **in**
685 **Supplementary Material Figure S8.**

686

687 **Figure 4.** Box plot of N/C ratio for deposited and suspended sediments (DS and SS), density-separated
688 sediment and end-member samples collected along the Abukuma River basin (i.e., terrestrial soils and
689 plants and riverine algae). Top, middle and bottom horizontal lines represent third quartile, median and
690 first quartile, respectively. Upper and lower whiskers represent maximum and minimum values,

691 respectively. The different letters (i.e., a, b, c and d) indicate significant difference at 5% level
692 according to Tukey's test. Detailed values for the data used in **Figure 4** are listed in **Tables S1, S2 and**
693 **S3**.
694
695 **Figure 5**. Relations between (a) organic C content and RCs concentration and (b) specific surface area
696 and RCs concentration for unseparated and density-separated samples. Unseparated samples are from
697 deposited sediment in 2012 and 2013 (DS2012 and DS2013) and density-separated samples are from
698 St. 2 Marumori in 2013. Symbols represent open circles for unseparated samples, gray diamonds for
699 density-separated heavy (>2.4 $g.cm^3$) and intermediate (1.8 – 2.4 $g.cm^3$) fractions and closed diamond
700 for density-separated light fraction (<1.8 $g.cm^3$). Values of R^2 and p and regression equation from
701 linear regression analysis (for all data [n= 19]) were also provided. The data in this figure were
702 reproduced by using the data from **Figure 1** (for unseparated samples) and **Figure 2** (for density-
703 separated samples).

704 **Figure 1**

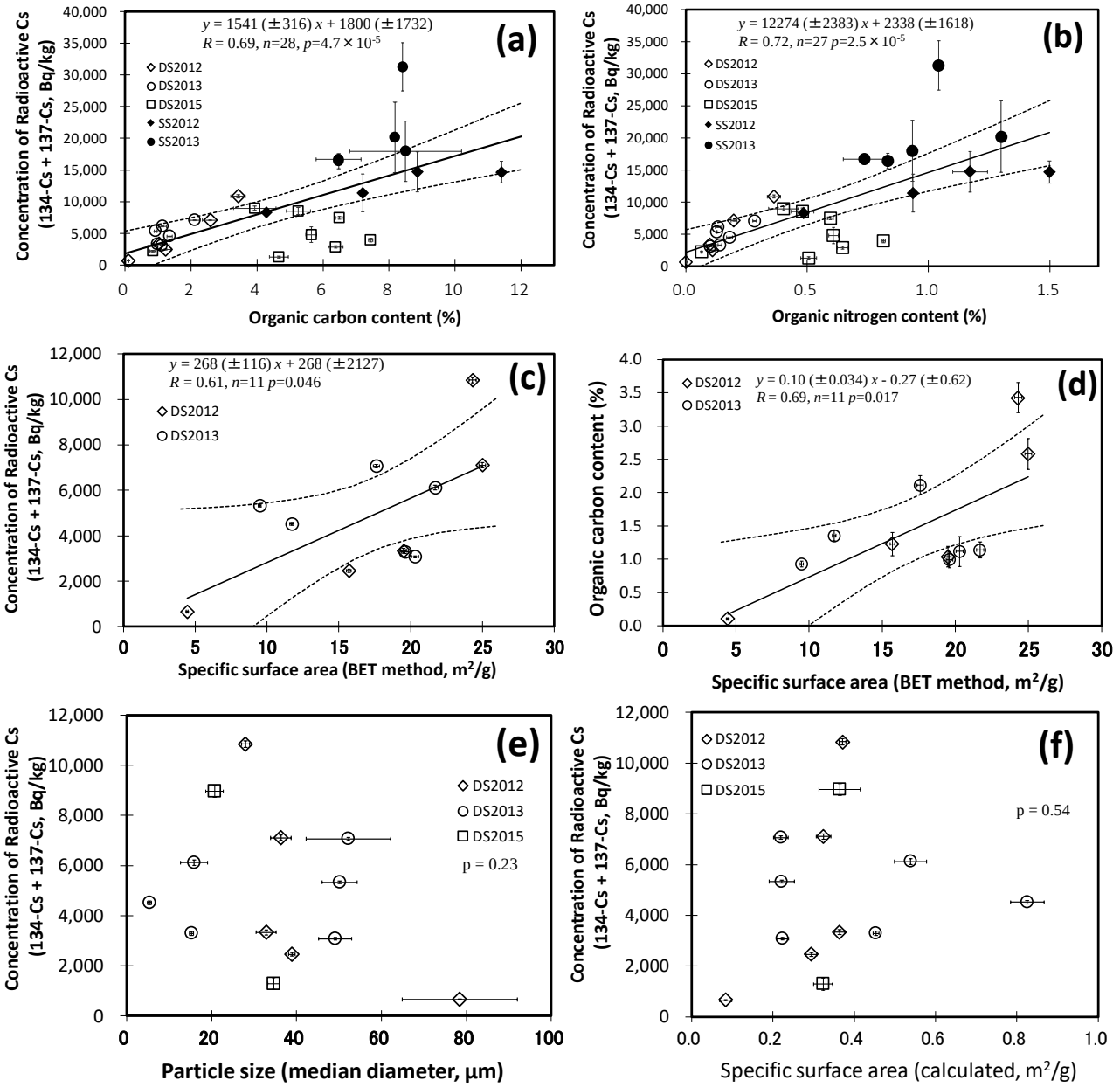

705

706

Figure 2

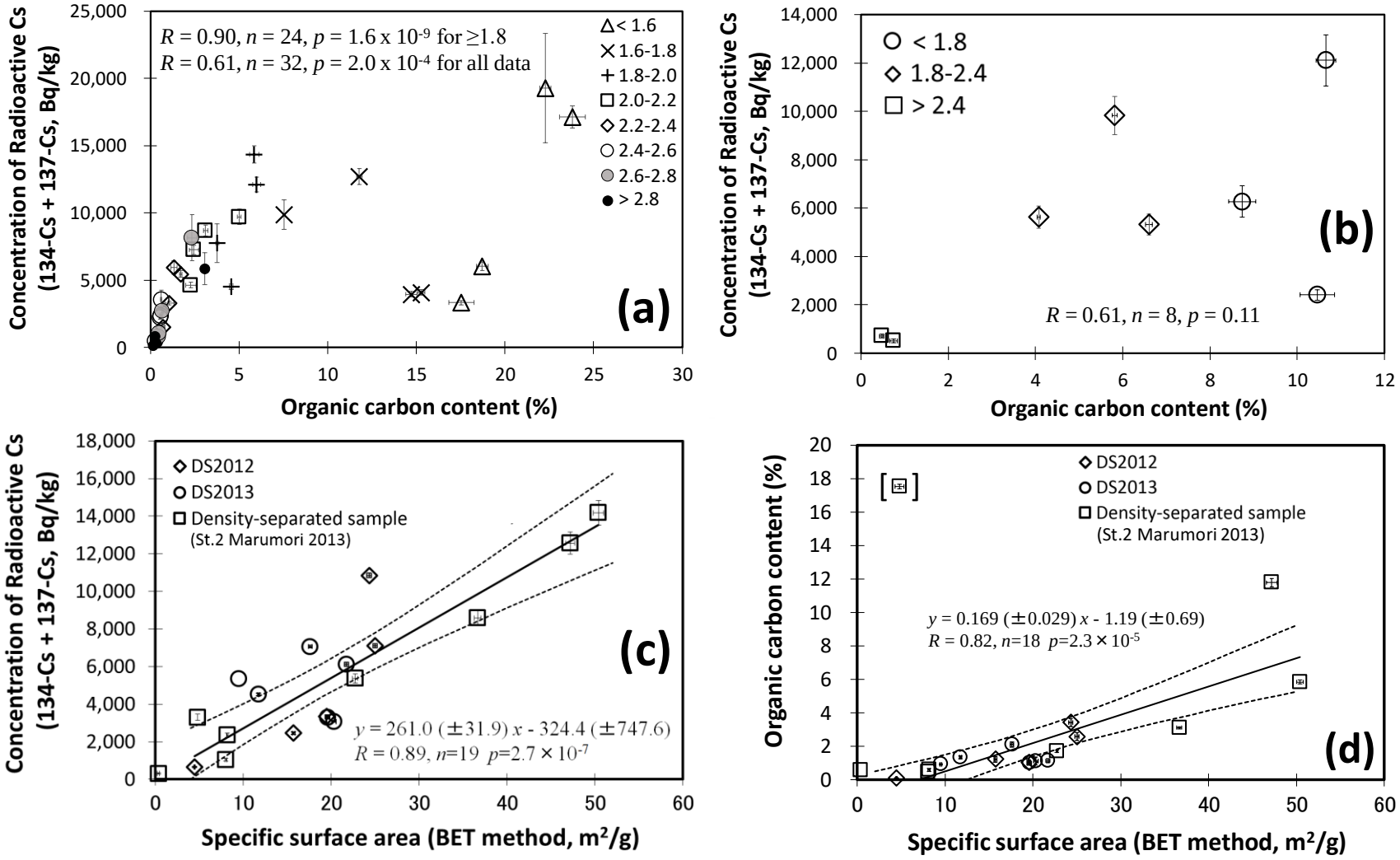
Concentration of Radioactive Cs (134-Cs + 137-Cs, Bq/kg)
Organic carbon content (%)
R = 0.90, n = 24, p = 1.6 x 10-9 for ≥1.8
R = 0.61, n = 32, p = 2.0 x 10-4 for all data
< 1.6
1.6-1.8
1.8-2.0
2.0-2.2
2.2-2.4
2.4-2.6
2.6-2.8
> 2.8
(a)
< 1.8
1.8-2.4
> 2.4
R = 0.61, n = 8, p = 0.11
(b)
DS2012
DS2013
Density-separated sample
(St.2 Marumori 2013)
y = 261.0 (±31.9) x - 324.4 (±747.6)
R = 0.89, n=19 p=2.7 × 10-7
(c)
Specific surface area (BET method, m²/g)
Organic carbon content (%)
y = 0.169 (±0.029) x - 1.19 (±0.69)
R = 0.82, n=18 p=2.3 × 10-5
(d)

Figure 3

a2. Marumori 2013: <1.6g/cm^3

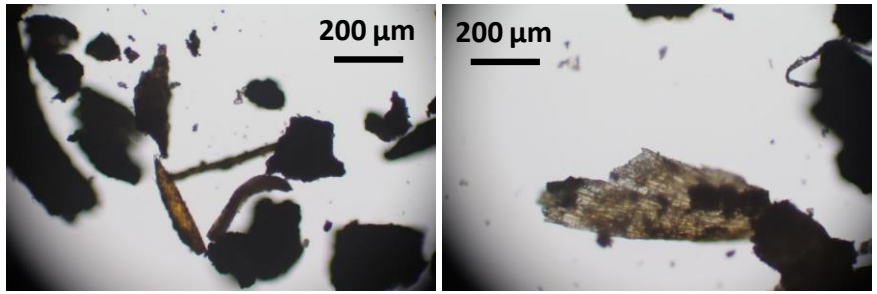

b1. Marumori 2013: 1.6-1.8g/cm^3

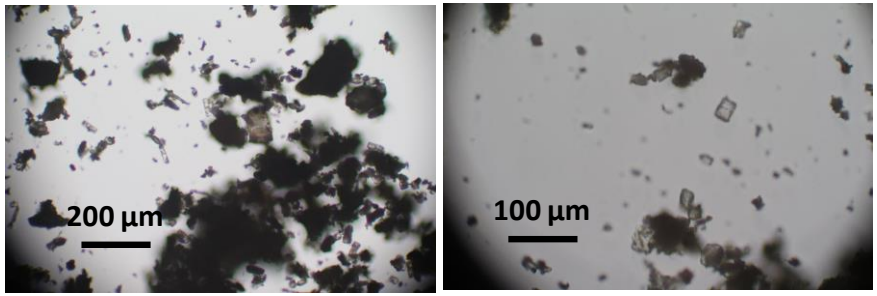

d1. Marumori 2013: 2.0-2.2g/cm^3

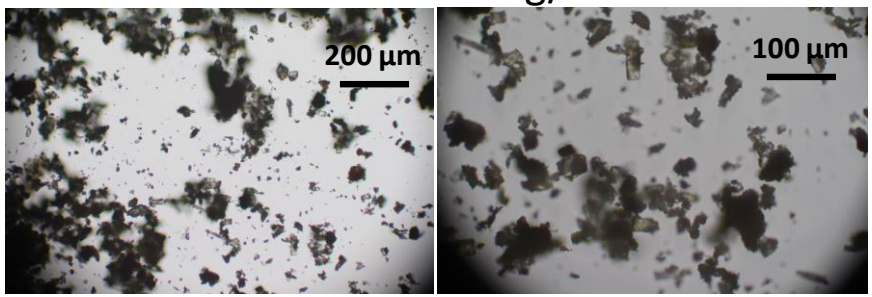

g1. Marumori 2013: 2.6-2.8g/cm^3

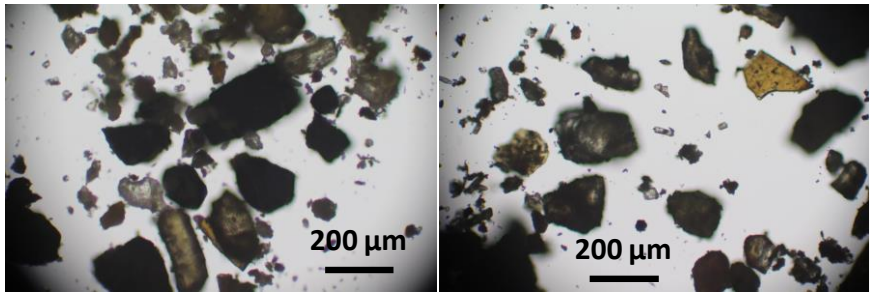

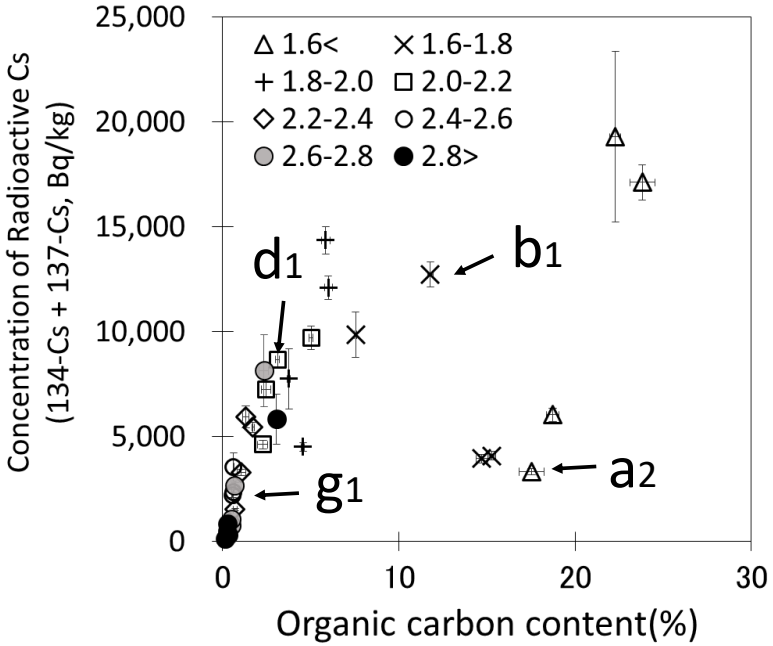

Figure 4

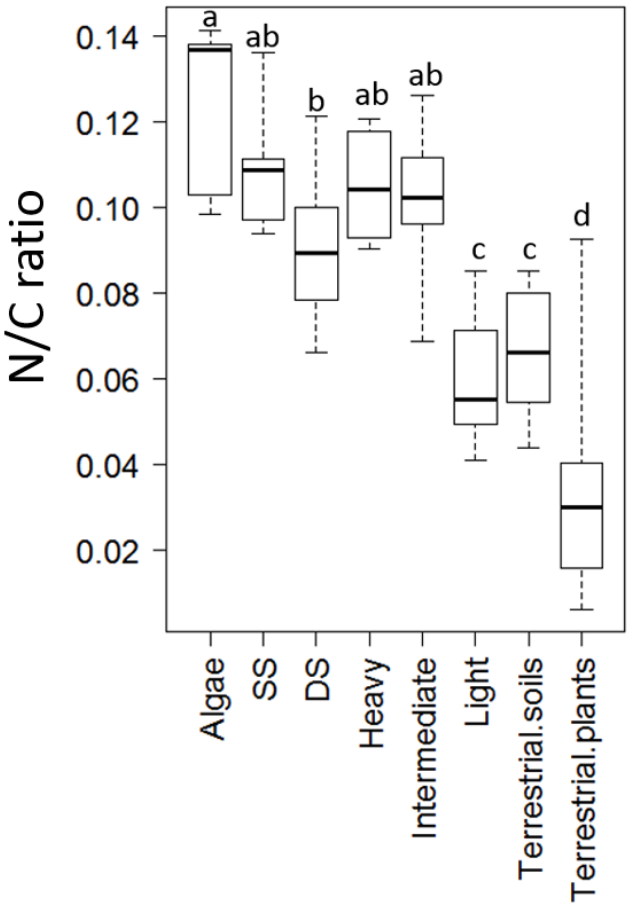
N/C ratio
0.14
0.12
0.10
0.08
0.06
0.04
0.02
a
ab
b
ab
ab
c
c
d
Algae
SS
DS
Heavy
Intermediate
Light
Terrestrial.soils
Terrestrial.plants

Figure 5

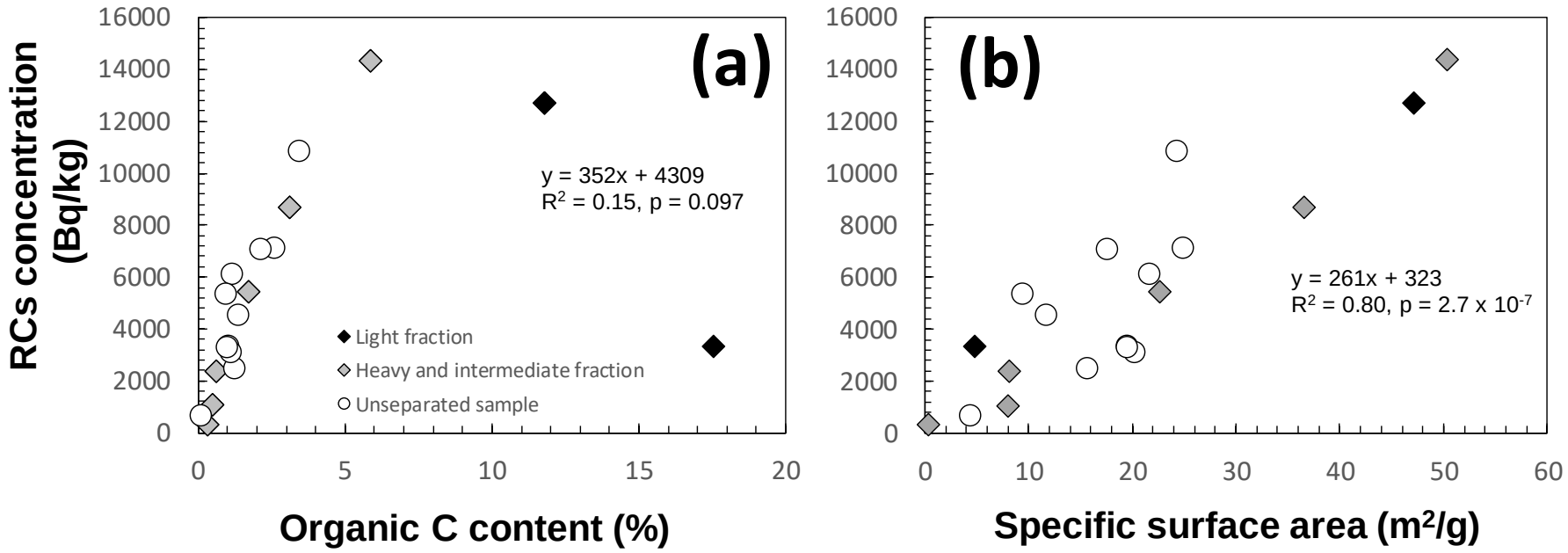
(a)
(b)
RCs concentration (Bq/kg)
Organic C content (%)
Specific surface area (m²/g)
y = 352x + 4309
R² = 0.15, p = 0.097
y = 261x + 323
R² = 0.80, p = 2.7 x 10⁻⁷
Light fraction
Heavy and intermediate fraction
Unseparated sample
0
2000
4000
6000
8000
10000
12000
14000
16000
0
5
10
15
20
0
10
20
30
40
50
60